Published in Medical Engineering and Physics26(8):pp.655-662.

Finite Element Modeling of the Contact Interface Between Trans-Tibial Residual Limb and Prosthetic Socket

Winson C.C. Lee [a], Ming Zhang [a,*], Xiaohong Jia [a,b], Jason T. M. Cheung [a]

[a] Jockey Club Rehabilitation Engineering Centre, The Hong Kong Polytechnic University, Hong Kong, China
[b] Department of Precision Instruments, Tsinghua University, Beijing 100084, China

* Correspondence address:

Ming Zhang (PhD)
Jockey Club Rehabilitation Engineering Centre,
The Hong Kong Polytechnic University,
Hung Hom, Kowloon, Hong Kong, P.R. China.
Tel: 852-27664939
Fax: 852-23624365
Email: rcmzhang@polyu.edu.hk

Abstract – Finite element method has been identified as a useful tool to understand the load transfer mechanics between a residual limb and its prosthetic socket. This paper proposed a new practical approach in modeling the contact interface with consideration of the friction/slip conditions and pre-stresses applied on the limb within a rectified socket. The residual limb and socket were modeled as two separate structures and their interactions were simulated using automated contact methods. Some regions of the limb penetrated into the socket because of socket modification. In the first step of the simulation, the penetrated limb surface was moved onto the inner surface of the socket and the pre-stresses were predicted. In subsequent loading step, pre-stresses were kept and loadings were applied at the knee joint to simulate the loading during the stance phase of gait. Comparisons were made between the model using the proposed approach and the model having an assumption that the shape of the limb and the socket were the same which ignored pre-stress. It was found that peak normal and shear stresses over the regions where socket undercuts were made reduced and the stress values over other regions raised in the model having the simplifying assumption.

Keywords: automatic contact, finite element analysis, interface pressure, pre-stress, prosthetic socket, shear stress

INTRODUCTION

A lower-limb prosthetic socket provides coupling between the residual limb and prosthesis. The biomechanical understanding of their mechanical interaction is fundamental to achieve a successful prosthesis fit (1). Finite element (FE) methods have been identified as a useful tool to understand the load transfer mechanics between the residual limb and prosthetic socket (2-14). The previous FE analyses have provided a better understanding of the effects of socket modifications (2,3), material properties of the sockets (2,7) and liners (2,8), alignment (3,4), residual limb geometry (2) and mechanical properties (2,3), and frictional properties at the interface (5) on the stress distribution over the residual limb. FE analyses can offer prediction of stress, strain and motion at any locations of the model and proficient parametric studies (9). However, the accuracy and efficiency of a model depend on the model establishment and parameters assigned.

In FE modeling of lower-limb prosthesis, simulation of the contact between the limb and socket is a great challenge because there is frictional/sliding action at the interface and the residual limb is donned into a socket with a different shape from the naked residual limb surface. In previous models, assumptions were made to simplify the problem. One simplification is that the residual limb and prosthetic socket are fully connected as one body assigned with different mechanical properties (2,3,4,7,10,11). This will reduce the difficulties of modeling and computational time; however, this prevents any slippage at the interface and large in-plane stresses might develop at the limb surface. Another commonly adopted assumption is that the shapes of the residual limb and rectified socket are the same (3,4,7,10-12). Under this assumption, the socket shape modifications aiming to redistribute the load to load-tolerant regions cannot be implemented in the FE prediction. The stresses applied onto the residual limb after donning into the rectified socket, defined as pre-stresses in this paper, were ignored under the above assumption.

Zhang and his colleagues (5) introduced interface elements to simulate the friction/slip conditions at the interface. The socket and residual limb were treated as separate bodies and interface elements were added between the two bodies. Shear stresses between the contact bodies can be analyzed with a given coefficient of friction. Slipping was allowed if the shear stress exceeded the frictional limit. However, uses of interface elements have to enforce point-to-point correspondent connections between the limb surface and the inner surface of the socket. An automated contact method was proposed by Zachariah and Sanders (12). The residual limb and prosthetic socket can be modeled as two deformable bodies in contact. The contact was simulated by automatically detecting any overlapping of interface nodes and imposing a non-penetration condition constraint to the overlapped nodes. However, this model did not implement the simulation of the interaction and pre-stresses produced by donning the residual limb into the rectified socket.

Simulation of donning the residual limb into a rectified socket has been implemented in some models by applying radial displacements to the nodes of the unrectified socket to deform it into the rectified socket shape (2,3,5,13,14). This method has been compromised with model building time because all the nodes at the areas which require shape modifications have to be identified and changes of coordinates imposed. It is difficult to implement this with auto-meshing techniques in model development. In many commercial FE packages, there is a limitation that only tetrahedral elements can be used in auto-meshing for geometrically irregular structures such as the residual limb. This auto-meshing process can result in a disorganized nodal arrangement and it is not convenient to identify the nodes for applying

radial displacement.

The objective of this paper is to propose a new technique to simulate the contact at the limb-socket interface using an automated contact method. The new technique can consider both the frictional/slipping conditions and pre-stresses produced by donning the limb into the rectified socket. The differences in interface stress distribution between the model using the new technique and the model assuming that the shape of the limb and the socket were the same ignoring pre-stress were also investigated.

METHODS

Geometries

The geometries of the residual limb surface and the internal bones were captured from a male trans-tibial amputee, 56 years old, 158cm tall and 81kg in mass who had more than 25 years experience using his prosthesis with a patellar-tendon-bearing (PTB) socket and a SACH foot. Magnetic resonance images (MRI) were obtained from the residual limb in supine lying and knee extended position with axial cross-sectional images at an interval of 6mm. To reduce the distortion of the soft tissues at the posterior regions, the subject wore an unrectified socket, based on a loose plaster cast on the limb surface, during the scanning procedure. The bones and the limb surfaces were identified and segmented using software Mimics v7.1 (Materialise, Leuven, Belgium).

The unrectified cast, representing the residual limb surface, was digitized and exported to prosthetic computer-aided design (CAD) software ShapeMaker 4.3 (Seattle Limb System). This shape would be modified into a PTB socket. A rectification template, shown in **Figure 1,** was applied by a prosthetist onto this shape by adding build-ups at pressure-sensitive areas and undercuts at pressure-tolerant areas to prepare the inner surface of the rectified socket. The socket was designed such that there would be no distal end support.

The surfaces of the bones, residual limb and socket were imported to SolidWorks 2001 (SolidWorks Corporation, Massachusetts). There were two sets of geometries and both sets contained the residual limb surface. The bones and residual limb exported from Mimics were aligned according to MRI and the socket and residual limb exported from ShapeMaker were aligned such that the socket build-ups and undercuts corresponded to the pressure sensitive and insensitive areas of the limb respectively. As shown in **Figure 2**, there were some areas overlapped at the interface where socket undercuts were made. Assembling of socket, limb and bones were done by moving the bones and limb surface as a whole inside the socket such that two limb surfaces coincided.

The surfaces were then converted into solid models using SolidWorks. The soft tissue model was generated by geometrically subtracting the bones from the limb solid. The socket has a thickness of 4mm. The solid models representing bones, soft tissues and rectified socket were then imported to the finite element package ABAQUS version 6.3 (Hibbitt, Karlsson & Sorensen, Inc., Pawtucket, RI). A FE mesh with a total of 22,301 3D tetrahedral elements was built using ABAQUS auto-meshing techniques. The meshed geometries of residual limb, prosthetic socket and bones are shown in **Figure 3.**

Material properties

The mechanical properties of the materials were assumed to be linearly elastic, isotropic and homogeneous. The Young's modulus was 200kPa for soft tissues and 10GPa for bones.

Poisson's ratio was assumed to be 0.49 for soft tissues and 0.3 for bones (5). The socket was assigned with Young's modulus of 1500MPa and Poisson's ratio 0.3, resembling the mechanical property of polypropylene homopolymer.

Boundary conditions and analysis steps

The external surface of the socket was fixed. The bones and soft tissues were modeled as one body with different mechanical properties. The residual limb and socket were modeled as two separate structures and their interaction was simulated using automated contact methods. The inner surface of the socket and the residual limb surface were defined as master and slave surfaces respectively. The contact simulation offered in ABAQUS (15) is described as follows (**Figure 4**). Normal vectors, e.g. $N_{2,}$ are computed for all nodes on the master surface by averaging the normal vectors of outward edges (1-2 and 2-3 segments) making up the master surface and additional normal vectors, e.g. $N_{L/2}$, are computed at the middle of each segment. Those normal vectors together with the element size and function are used to define a set of smooth varying normal vectors on the whole master surface. An "anchor" point on the master surface X_0 is calculated for each node on the slave surface (slave node) so that the vector formed by the slave node and X_0 coincided with the normal vector $N(X_0)$ of the master surface. A tangent plane is found out at every "anchor" point which is perpendicular to the normal vector. Under the strict master-slave contact algorithm in ABAQUS, the slave nodes are automatically constrained not to penetrate into their tangent planes on the master surface when two surfaces come into contact.

There were two analysis steps. The first step was to establish the pre-stress condition from donning the limb into the rectified socket. At this step, an axial force of 50N was applied at center of the knee joint to approximate the force stabilizing the limb in the socket. Shear stress was assumed to be zero in this step because there was little tendency of the limb sliding. Initially, some nodes on the slave surface (limb surface) penetrated into the master surface (inner surface of the socket) because of the socket rectifications. Under the master-slave contact algorithm in which no penetration of slave nodes into the master surface is allowed, the solver in ABAQUS (15) moved the penetrating slave nodes onto their corresponding tangent planes of the master surface, as displayed in **Figure 5**. Stresses were developed at both the master and slave surfaces over the overlapping regions.

At the second step, the pre-stresses and the deformations calculated in the first step were kept and external loading was applied at the knee joint. Three load cases **(Figure 2)** were applied separately to simulate the loading conditions at foot flat, mid-stance and heel off during walking. Using inverse dynamics, the loads applied at the knee joint were calculated from kinematic data of the prosthesis measured by Vicon Motion Analysis System, the ground reaction forces measured by a force platform of the same subject during walking (16, 17, 18) and the anthropometric data of the lower limb of the subject. It was assumed in the FE model that the knee joint angle did not change at different loading cases. The assumption was made because 1) loads were added at the knee joint so that the directions of loads were not affected by the lack of knee flexion, 2) soft tissues around the femur did not contact with the prosthetic socket and 3) the prediction of the shape and volume of soft tissues around the femur from extended to flexed knee position could be difficult. There were no artificial constraints imposed between the master and slave surfaces when they were separated as no interface elements were defined at the interface. When the nodes on the slave surface contacted with their corresponding tangent planes of the socket, the solver constrained those nodes not to penetrate into the tangent planes and stress was developed at both master and slave surfaces. Coefficient of friction (μ) of 0.5 was assigned for the socket-limb interface (5, 19). During

the contact phase, sliding was allowed only when the shear stress exceeded the critical shear stress value $\tau > \tau_{crit} = \mu p$, where p is the value of normal stress. During the sliding phase, if the shear stress was reduced and lower than the critical shear stress value, sliding stopped. It was assumed that the static and kinetic coefficients of friction were the same in this model.

To understand how the pre-stresses influence the predictions, a second model was built for comparison which was the same as the previous model except that the initial geometry of the residual limb was made the same as that of the rectified prosthetic socket and no pre-stress was applied onto the residual limb at the first analysis step. The shape change of the residual limb after socket donning was simulated in the second model, however, no pre-stress existed as there was no overlapping region between the limb and the socket at initial configuration.

RESULTS

Figures 6 (a) and (b) show the normal stress distributions predicted from the first step when the limb was donned into the socket. High normal stress was produced at the regions where socket undercuts were made, including patellar tendon (96kPa), popliteal depression (147kPa), anteromedial tibial (52kPa) and anterolateral tibial (84kPa). **Figure 6** (c) and (d) display the normal stress distribution obtained from the second step analysis when loadings simulating mid-stance were applied with pre-stress considered. The normal stresses over regions where socket undercuts were made further increased, up to a maximum of 185 kPa over the mid-patellar tendon region. As the Young's modulus of the socket was much higher than that of soft tissues and there was no direct contact between the socket and the bones, the deformation of the socket was negligible.
Figure 7 (a) and (b) shows the resultant shear stress distribution at the limb/socket interface when loadings simulating mid-stance were applied with pre-stress considered. The resultant shear stress is the magnitude of the combination of longitudinal and circumferential components of shear stresses in the plane of contact interface. High resultant shear stresses were predicted at the four critical regions where socket undercuts were made. The maximum value is 67kPa over the patellar tendon region.

Figure 8 shows the comparison of the peak normal stresses and peak resultant shear stresses over the four regions at the three walking phases. Relatively larger increases of normal stress from pre-stress to foot flat over the patellar tendon region and from pre-stress to heel off at the anterolateral tibial and popliteal depression regions were noted. The large increases were due to the flexion and extension moment of the limb relative to the fixed socket caused by body weight predominantly.

Stresses distribution patterns over the residual limb and peak stress values over the four pressure-tolerant regions were different in the second model which has a simplifying assumption that the shape of limb and the rectified socket were the same ignoring pre-stress. **Figure 6** (e) and (f) shows the normal stress distribution and **figure 7** (c) and (d) shows the resultant shear stress distribution over the limb at mid-stance at the second model. Stresses were more evenly distributed in the second model. Peak normal and resultant shear stresses were lowered over the four pressure-tolerant regions where socket undercut regions were made but higher stresses fell on regions which are not pressure-tolerant.

DISCUSSION AND CONCLUSIONS

Zachariach and Sanders (12) used an automated contact method to simulate contact between

the limb and the socket in previous model. In that model, the shapes of the limb and rectified socket were assumed to be the same so that the effect of pre-stresses was not considered. The same automated contact method was used in this investigation to study the stress distribution during walking with pre-stress considered. Due to the difference in limb and socket shape, there were some regions of the limb which penetrated into the socket at the initial configuration. The penetrated limb surface was automatically deformed such that it just contacted the inner surface of the socket. At subsequent stages when loadings were applied simulating three load cases during stance phase of the gait, the limb surface was constrained automatically not to penetrate the socket inner surface. The limb was allowed to slide if the shear stress exceeded the frictional limit.

The difference in shape between the residual limb and socket imposes challenges in contact simulation at the limb-socket interface. Simplification was usually made assuming that the limb and socket had the same shape, however, pre-stress was ignored which could lead to inaccuracy of the model. In this investigation, it was shown that peak normal and shear stresses over patellar tendon, anterolateral and anteromedial tibia and popliteal depression would have noticeable decreases if the simplifying assumption that, the shape of the residual limb and the rectified socket were the same, was imposed.

In some previous models, socket modification was done by radial nodal displacement method. The socket was initially the same as that of the residual limb obtained from imaging methods. Socket modification and pre-stresses were introduced by manually input the displacement to each node at the selected regions of the socket in FE analysis package to deform it into rectified socket and the residual limb. In this investigation, socket rectifications were performed in prosthetic CAD software ShapeMaker by applying a build-in template to the digitized unrectified socket surface. ShapeMaker together with computer aided manufacturing machine are commonly used in clinical practice to design and fabricate prosthetic socket. Clinicians are required to mark the locations of some important landmarks such as patellar tendon and fibular head. A build-in template, which reads the marked landmarks and automatically performs vectors operations at the regions around the landmarks, is applied. Subsequent minor modification, such as changing the degree of undercuts and the area of modification, can be performed manually in CAD based.

The real procedure of socket donning was not simulated in this investigation. Instead, the final deformation state of the limb immediately after donning into a socket was studied. Simulation of socket donning is challenging because donning involves wiggling and large relative motions which are difficult to define. If the wiggling motions are not simulated and the limb is forced straight into the socket, severe distortions of the limb could happen due to the complicated shape of the socket. Large sliding action between the limb and the socket requires significant computational resources. Some of the latest models have tried to simulate the donning process by applying axial displacement to the residual limb with the socket fixed or to the socket with the limb fixed (8, 20). Those models, however, over-simplified the geometry of the residual limb and socket such that the wiggling motion of the limb was ignored during the donning process.

A liner was not added in this FE model. Liners can help distribute stress more evenly throughout the residual limb and could increase the chance of successful prosthesis fitting. However, they could also produce some troubles to the patients which include hygiene problems (sweat absorbing), requirement of frequent maintenance of liners and the prosthetic socket will become more bulky and less cosmetic after the insertion of liner. The authors of

this paper are engaged to optimize the design of a monolimb (a prosthesis with its socket and shank molded into one piece of thermoplastic) offering low-cost and easy fabrication to patients and clinicians particularly in developing countries. We have some experience of fitting patients with monolimbs which do not have liners and we do not encounter major fitting problems. The model presented in this manuscript will be modified and used to aid design of monolimbs. For these reasons a liner was not added.

Future FE analysis will be performed using the new technique to model residual limb and monolimb. The effect of different design parameters such as socket shape-modification method, shank and prosthetic foot stiffness on the stress distribution at the limb/socket interface will be studied. More accurate description of material properties of soft tissues especially on their non-linear material properties will be pursued. In addition to stress distribution at the limb-socket interface, stress tolerant ability of different regions of the residual limb is critical in socket design and fit. High stresses applied onto the residual limb which is not particularly tolerant to loadings is the cause of the pain. FE modeling can display the stress distribution over the residual limb during walking. However, without an adequate understanding how tissues at various sites respond to stresses, it is difficult to discuss the optimal stress patterns over the stump. The amount of stress that the soft tissues of different regions can tolerate requires exploration.

ACKNOWLEDGEMENTS

The work described in this paper was supported by The Hong Kong Polytechnic University Research Studentship and a grant from the Research Grant Council of Hong Kong (Project No. PolyU 5200/02E). We would like to acknowledge the Scanning Department of St. Teresa's Hospital, Kowloon, Hong Kong for the MR scanning.

REFERENCES

1. MAK AFT, ZHANG M, BOONE DA, State-of-the-art research in lower-limb prosthetic biomechanics - socket interface. J Rehab Res Dev 2001;38: 161-74.
2. SILVER-THORN MB, CHILDRESS DS. Parametric analysis using the finite element method to investigate prosthetic interface stresses for persons with trans-tibial amputation. J Rehab Res Dev 1996;33: 227-38.
3. REYNOLDS DP, LORD M. Interface load analysis for computer-aided design of below-knee prosthetic sockets. Med & Biol Eng & Comput 1992;30: 419-26.
4. SANDERS JE, DALY CH. Normal and shear stresses on a residual limb in a prosthetic socket during ambulation: comparison of finite element results with experimental measurements. J Rehab Res Dev 1993;30: 191-204.
5. ZHANG M, LORD M, TURNER-SMITH AR, ROBERTS VC. Development of a non-linear finite element modeling of the below-knee prosthetic socket interface. Med Eng Phys 1995;17: 559-66.
6. ZHANG M, TURNER-SMITH AR, ROBERTS VC, and TANNER A, Frictional action at residual limb/prosthetic socket interface. Med Eng & Phys 1996;18: 207-14.
7. QUESADA P, SKINNER HB. Analysis of a below-knee patellar tendon-bearing prosthesis: a finite element study. J Rehab Res Dev 1991;28: 1-12.
8. SIMPSON G, FISHER C, WRIGHT DK. Modeling the interactions between a prosthetic socket, polyurethane liners and the residual limb in transtibial amputees using non-linear finite element analysis. Biomed Sci Instrum 2001;37: 343-47.
9. ZHANG M, MAK AFT, ROBERTS VC. Finite element modeling of a residual lower-limb in a prosthetic socket: a survey of the development in the first decade. Med Eng Phy 1998;20: 360-73.
10. STEEGE JW, SCHNUR DS, VANVORHIS RL, ROVICK JS. Finite element analysis as a method of pressure prediction at the below-knee socket interface. In: Proceedings of the 10th Annual RESNA conference, 1987, San Jose, CA. Washington, DC: RESNA Press, 1987:814-6.
11. STEEGE JW, SCHNUR DS, CHILDRESS DS. Prediction of pressure in the below-knee socket interface by finite element analysis. In: ASME Symposium on the biomechanics of Normal and Pathological Gait, 1987:39-44.
12. ZACHARIAH SG, SANDERS JE. Finite element estimates of interface stress in the trans-tibial prosthesis using gap elements are different from those using automated contact. J Biomech 2000; 33: 895-9.
13. ZHANG M, ROBERTS VC. Comparison of computational analysis with clinical measurement of stresses on below-knee residual limb in a prosthetic socket. Med Eng & Phys 2000;22: 607-12.
14. SILVER-THORN MB, CHILDRESS DS. Generic, geometric finite element analysis of the transtibial residua limb and prosthetic socket. J Rehab Res Dev 1997;34: 171-86.
15. ABAQUS User Manual (version 6.3), 2002, Hibbitt, Karlsson & Sorensen, Inc., Pawtucket, RI.
16. JIA XH, ZHANG M, LEE WCC. Dynamic effects on interface mechanics of residual limb/prosthetic socket system. In: Proceedings of the International Society of Biomechanics. Dunedin, New Zealand: 2003.
17. LEE WCC, ZHANG M, JIA XH, BOONE DA. A computation model for monolimb design. In: Proceedings of the International Society of Biomechanics. Dunedin, New Zealand: 2003.
18. JIA XH, ZHANG M, LEE WCC. Load transfer mechanics between trans-tibial prosthetic socket and residual limb – dynamic effects. J Biomech 2004, In press.
19. ZHANG M and MAK AFT. In *vivo* friction properties of human skin. Prosthet & Orthot

1999;23: 135-41.
20. FINNEY L. Simulation of donning a prosthetic socket using an idealized finite element model of the residual limb and prosthetic socket. In: Proceedings of the 10th International Conference on Biomedical Engineering, Singapore, 2000: 71-2.

CAPTIONS

Figure 1. Socket rectification template. Patella (Pa), patellar tendon (PT), fibular head (FH), anteromedial tibia (AMT), anterolateral tibia (ALT), tibial crest (TC), fibular end (FE), tibial end (TE) and popliteal depression (PD) are the regions where rectifications were applied. The numbers show the maximum depth/height (in millimeter) of undercuts (negative values) or build-ups (positive values) over the regions.

Figure 2. Assembled socket, limb and bone surfaces. Overlapping can be seen over patellar tendon and popliteal depression regions at the lateral view. Forces and moments were applied at the knee joint, as shown simulating foot flat, mid-stance and heel off. X, Y and Z are local axes relative to the bone axis such that in sagittal plane the Y axis and X axis are along and across the femur and the tibia.

Figure 3. FE Mesh of the residual limb, prosthetic socket and bones. Intersected mesh at patellar tendon, anteromedial and anterolateral region of the socket was due to overlapped nodes.

Figure 4. Master slave contact algorithm. Anchor point (X_0) and tangent plane are computed for every slave node based on the computed normal vectors. Each slave node (e.g. node 5) is constrained not to penetrate its tangent planes.

Figure 5. (**a**) Some slave nodes penetrating into the master surface at the initial configuration; (**b**) Master slave contact algorithm in ABAQUS moves the penetrated slave nodes onto their tangent planes on master surface and stress developed at the interface.

Figure 6. The anterior and posterior views of contact normal stress distribution (**a, b**) after socket donning; **(c, d)** with pre-stress considered and **(e, f)** with pre-stress ignored at mid-stance.

Figure 7. The anterior and posterior views of resultant contact shear stress distribution at mid-stance phase (**a, b**) with pre-stress considered, and (**c, d**) with pre-stress ignored.

Figure 8. (a) Peak normal stress and **(b)** peak resultant shear stress at patellar tendon (PT), anterolateral tibia (ALT), anteromedial tibia (AMT), and popliteal depression (PD) regions of the model with pre-stress considered.

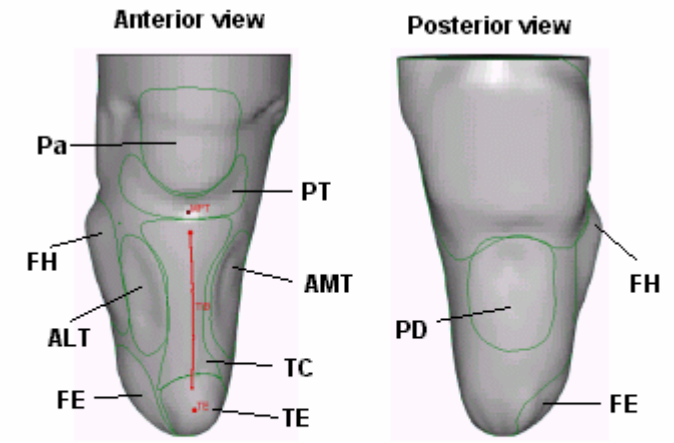

Pa	PT	FH	AMT	ALT	TC	FE	TE	PD
2	-7	7	-4	-3	3	4	7	-7

Figure 1

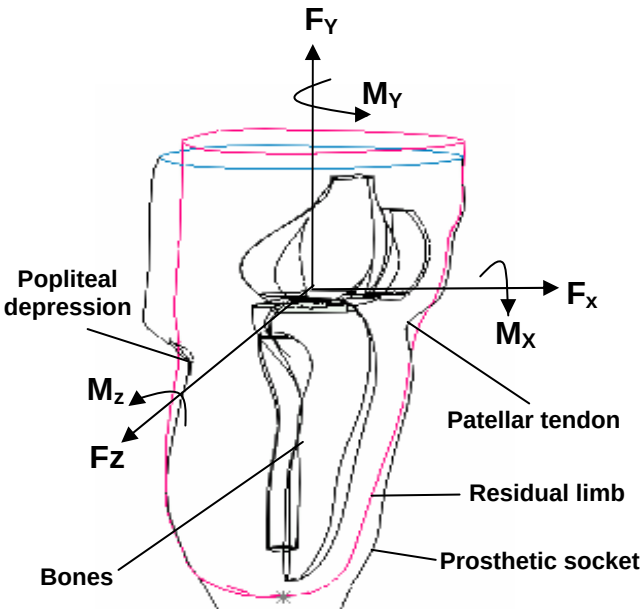

	Foot flat	Mid-stance	Heel off
F_x (N)	133	74	107
F_Y (N)	-923	-600	-757
F_z (N)	60	45	68
M_X(Nm)	20	11	16
M_Y(Nm)	-4	-1	1
M_Z(Nm)	-22	-0.7	23

Figure 2

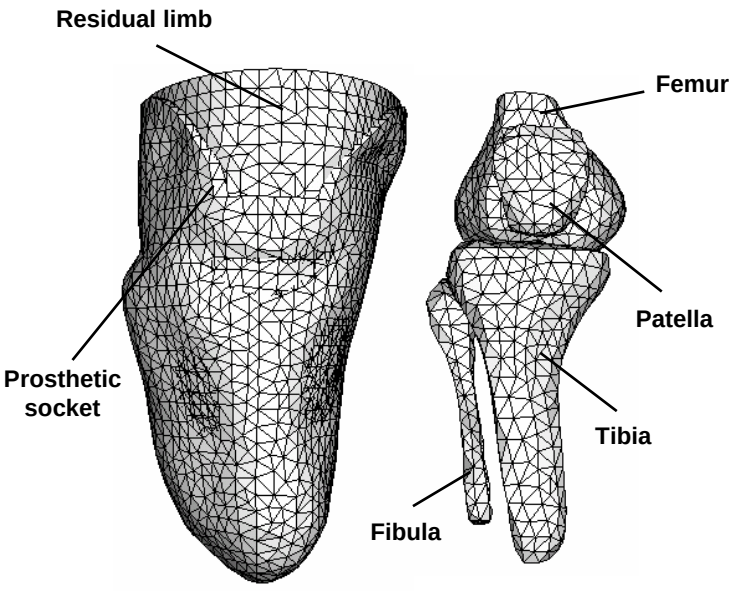
Residual limb
Femur
Patella
Prosthetic socket
Tibia
Fibula

Figure 3

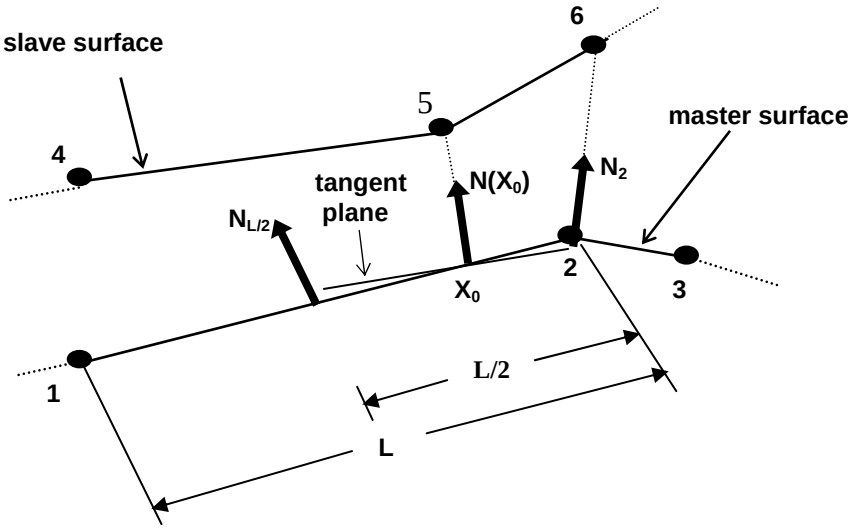
slave surface
6
5
master surface
4
tangent
plane
$N(X_0)$
N_2
$N_{L/2}$
2
X_0
3
1
L/2
L

Figure 4

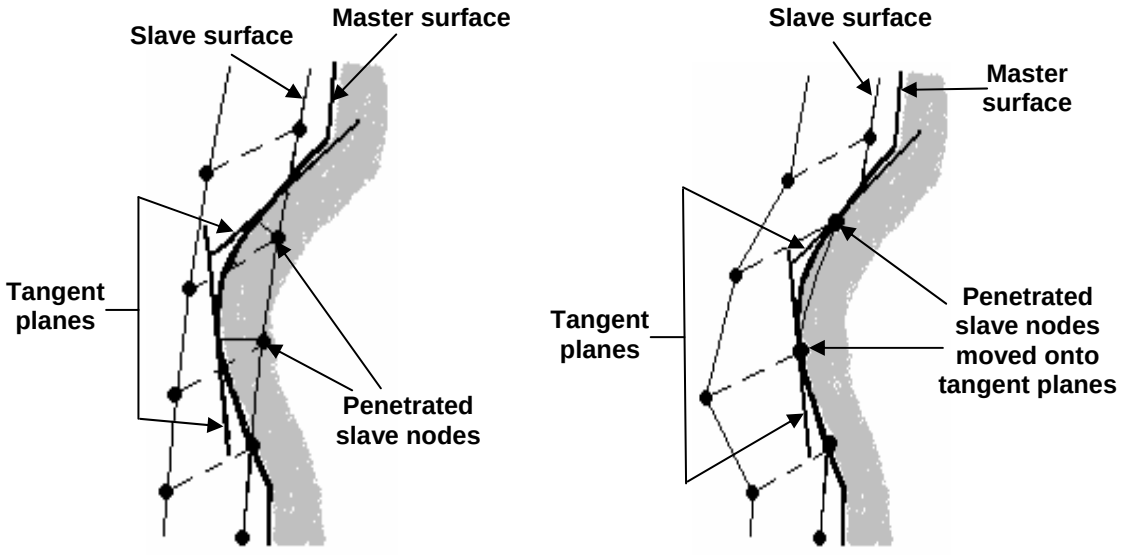
Slave surface
Master surface
Tangent planes
Penetrated slave nodes
(a)
Slave surface
Master surface
Tangent planes
Penetrated slave nodes moved onto tangent planes
(b)

Figure 5

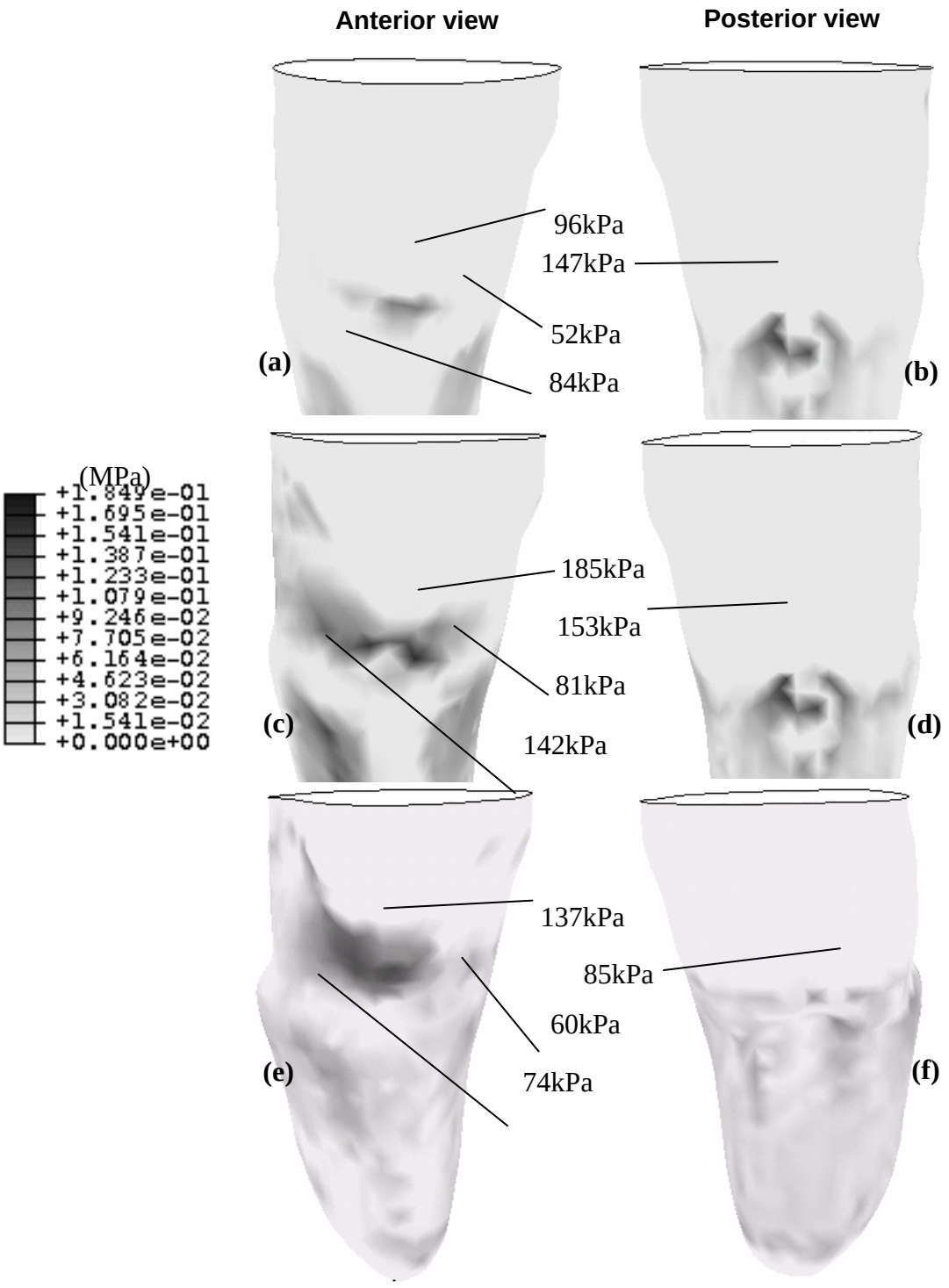
Anterior view
Posterior view
96kPa
147kPa
52kPa
84kPa
(a)
(b)
(MPa)
+1.849e-01
+1.695e-01
+1.541e-01
+1.387e-01
+1.233e-01
+1.079e-01
+9.246e-02
+7.705e-02
+6.164e-02
+4.623e-02
+3.082e-02
+1.541e-02
+0.000e+00
185kPa
153kPa
81kPa
142kPa
(c)
(d)
137kPa
85kPa
60kPa
74kPa
(e)
(f)

Figure 6

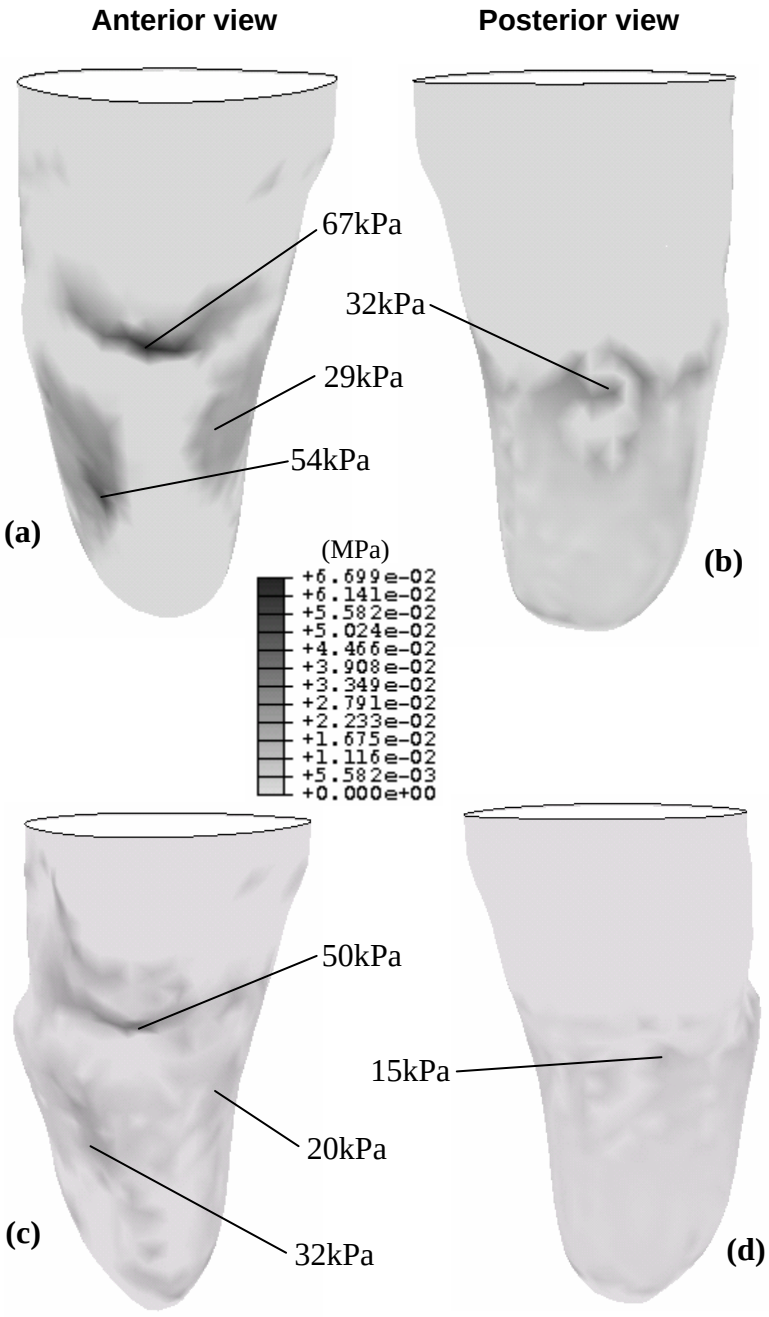
Anterior view
Posterior view
67kPa
32kPa
29kPa
54kPa
(a)
(b)
(MPa)
+6.699e-02
+6.141e-02
+5.582e-02
+5.024e-02
+4.466e-02
+3.908e-02
+3.349e-02
+2.791e-02
+2.233e-02
+1.675e-02
+1.116e-02
+5.582e-03
+0.000e+00
50kPa
15kPa
20kPa
32kPa
(c)
(d)

Figure 7

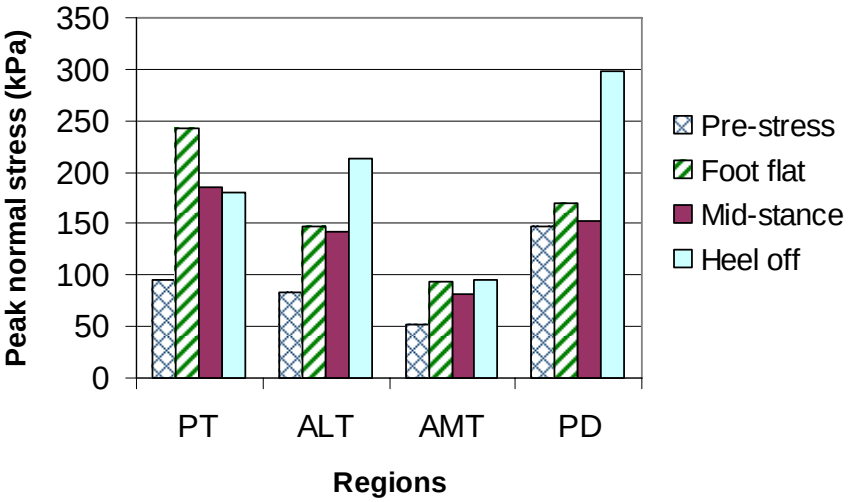
Peak normal stress (kPa)
350
300
250
200
150
100
50
0
PT
ALT
AMT
PD
Regions
Pre-stress
Foot flat
Mid-stance
Heel off

(a)

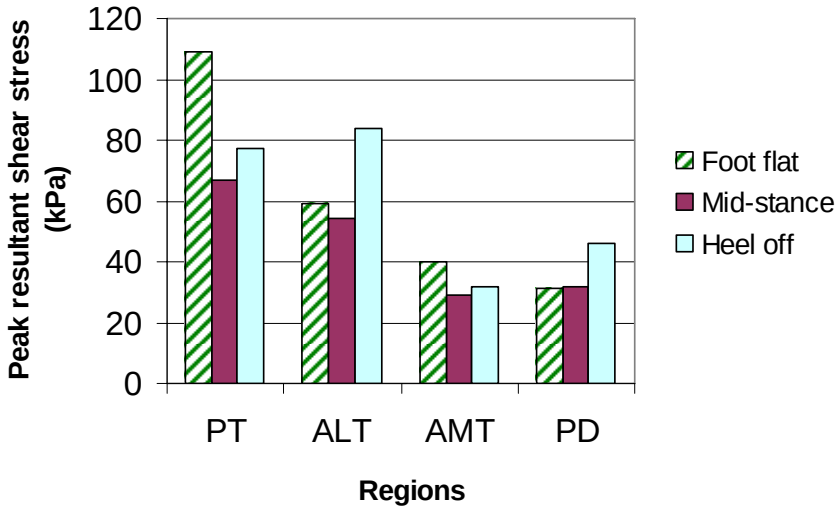
Peak resultant shear stress (kPa)
120
100
80
60
40
20
0
PT
ALT
AMT
PD
Regions
Foot flat
Mid-stance
Heel off

(b)

Figure 8